

ON THE USE OF EVENT-BASED CHANGE DETECTION NEUROMORPHIC IMAGERS FOR IN-PROCESS MONITORING OF ADDITIVE MANUFACTURING

David Mascareñas*, Andre Green*

*Engineering Division, Los Alamos National Laboratory, Los Alamos, NM 87545

Abstract

Imagers are attractive sensors for in-process monitoring of additive manufacturing (AM) processes on account of their ability to capture high spatial-resolution data. However, this advantage comes at the price of large memory generation. Additionally, some metallic AM processes have high light intensity and high speed dynamics which further complicates data collection. Emerging change detection, event-driven, neuromorphic imagers represent an alternate imaging modality. Change detection event imagers only report data for pixels whose log intensity value has changed beyond a specified threshold. These imagers tend to generate less data than conventional imagers, respond to sub-millisecond phenomena in the environment, and have a high dynamic range. These properties make these imagers attractive for a variety of AM processes. We demonstrate the performance of change detection event-based neuromorphic imagers in the context of AM/welding processes such as arc/laser welding.

Introduction

Currently in-process monitoring and imager-based documentation of additive manufacturing (AM) processes such as directed energy deposition (DED) and laser powder bed fusion (LPBF) is not practical over the course of the entire build of a part, on the shop floor. The primary challenge is that the dynamic phenomena present in wire directed energy deposition (W-DED) melt pools can take place on sub-millisecond timescales, thus requiring the use of imagers and other sensors with high sampling rates. This high sampling rates results in the generation of very large amounts of data at the point-of-manufacture. CEO/co-founder of the metal AM startup Freeform recently stated the scale of the data problem associated with additive manufacturing as “It's actually kind of crazy, the amount of data we move here...rivals like Netflix. [1].” This large amount of data (gigabytes to terabytes) requires impractically substantial computing resources to process on-line to enable real-time control. Furthermore, the amount of data generated per-part is on the order of terabytes, which quickly becomes impractical to store, and is difficult to transmit over Ethernet networks. This network transmission issue is particularly problematic. However, event-based, neuromorphic sensing and computing offers an alternative imaging measurement paradigm that has demonstrated great promise for efficiently and capturing data associated with the sub-millisecond dynamics of melt pools in high light intensity environments.

Neuromorphic event based imagers were originally proposed and developed by Carver Meade [2], [3], Misha Maldowald and Tobi Delbruck [4]. The idea behind this work was to look to the biological nervous system to inform the development of efficient sensing and computing. The event imager which was a precursor to the event imagers used in this work was developed by Lichtsteiner et al [5]. A review of event-based imaging can be found in [6]. Neuromorphic imagers are fundamentally different than conventional imagers. An event based imager does not capture individual photographs or frames. Instead, an event based imager only detects information associated with a change in light intensity value at an individual pixel. Furthermore, this event detection is done directly in hardware at the pixel level [5]. It must be stressed that the event detection is not the result of an image processing algorithm performed on a conventional image. The data for each event consists of an event timestamp that typically has ~10s of microseconds accuracy [7] as well as the x-y position of the pixel that detected the event and a polarity value which indicates if the pixel detected an increase or decrease in light intensity. Data is only reported from the imager, if the light intensity level at a given pixel changes. Furthermore, only the pixels whose light intensity value has changed, report data. If the pixel event data is arranged into the form of a photograph, the resulting data displays some similarity to a conventional image that has been processed using an edge detection algorithm. This detection-at-the-pixel approach, results in event-based sensors

consuming less power, less memory/bandwidth, and they operate across a wide range of timescales and dynamic ranges [5]. Event-based imagers also have the advantage that they effectively adaptively sample the field-of-view of the scene on a per-pixel basis based on the timescales at which changes in the scene are evolving. To demonstrate these properties of an event-based imager, consider the case of observing two propellers (Figure 1) spinning side by side, but at different rotational speeds. For this case, the spatio-temporal point cloud of events resulting from this observation is shown in Figure 2. A propeller sweeps out a corkscrew-shaped set of events as it progresses through time. The rate of periodicity associated with this corkscrew shape depends on the rotational speed of the propeller. Figure 2 clearly demonstrates that two different periods associated with the different rotational speeds of the propellers can be observed in Figure 2. This result illustrates that events are generated at a rate commensurate with the dynamics being observed by each individual pixel. Furthermore, only noise events are observed at pixels not observing a physical phenomena that results in changes in light intensity.

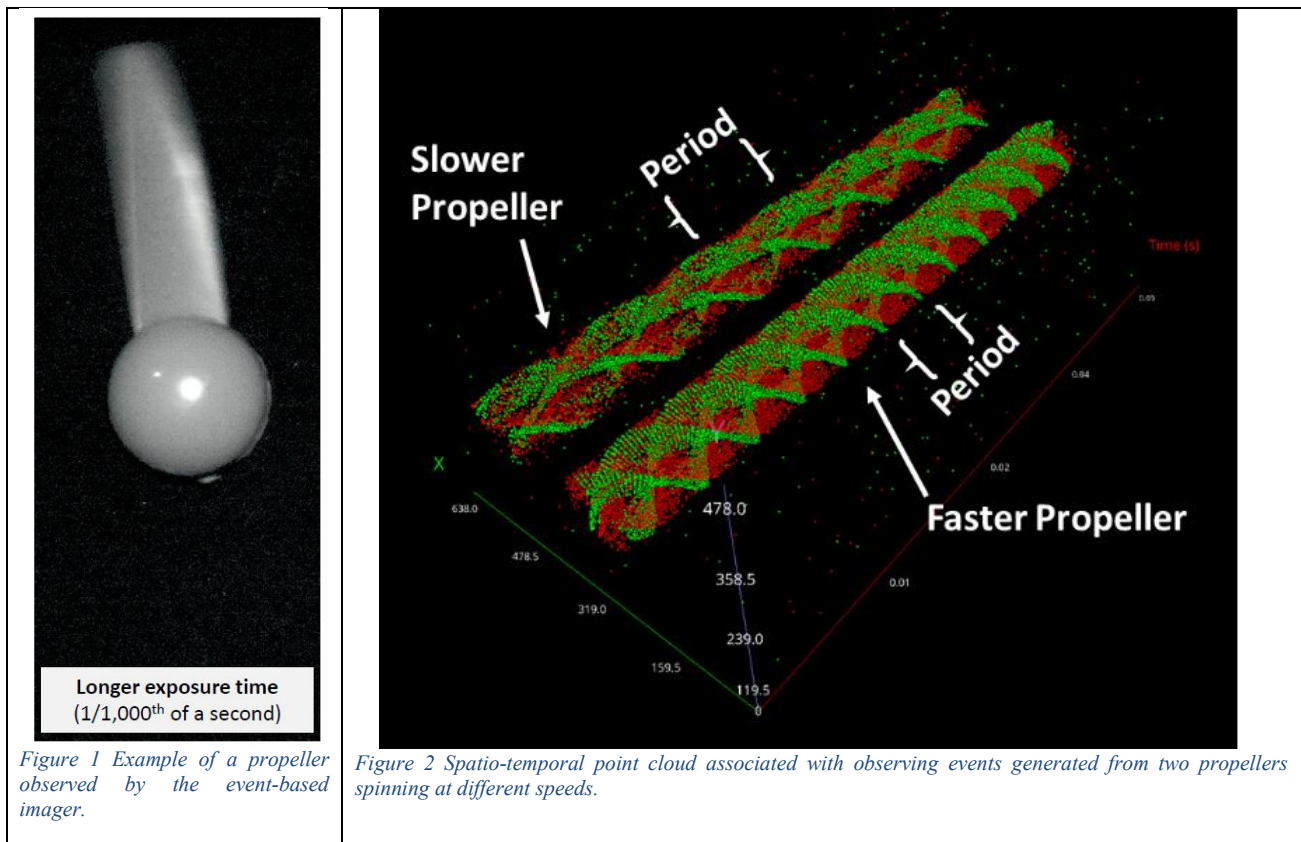


Figure 1 Example of a propeller observed by the event-based imager.

Figure 2 Spatio-temporal point cloud associated with observing events generated from two propellers spinning at different speeds.

One of the properties of event imagers that makes them particularly attractive for welding and additive manufacturing monitoring applications is the fact that they are often designed to detect events based on changes in the logarithm of the light intensity observed at a pixel [5]. As a result, these imagers tend to have dynamic ranges on the order of 120 dB [7], [8], [9] which corresponds to a 20 bit imager. In contrast, a conventional 8 bit imager only has 48 dB of dynamic range and a 12 bit imager has 72 dB of dynamic range. To demonstrate the high-dynamic range properties of event imagers, consider the case of observing an eclipse using an event-based imager as shown in Figure 3a. In this scene both a hand and the crescent sun shape associated with the eclipse can be observed simultaneously. The hand and the sun can be observed simultaneously in this case because each pixel detects changes in light intensity independently of the other pixels. As a result both very bright and significantly less bright objects can be observed simultaneously. In contrast Figure 3b. shows the eclipse and hand viewed using a conventional 8-bit imager. In this image it is not possible to observe the hand in the presence of the intense light radiated by the sun. This example drives home the extreme dynamic range achievable with event-based imagers.

To further illustrate the generation of event data to changes in log light intensity, consider the case of an event imager (DVXplorer [7]) observing a pin hole backlit with a light source that can be modulated illuminated through an integrating sphere. In this case the event imager observes the pinhole as the light source’s intensity is increased in an exponential manner. The resulting events from 9 neighboring pixels are then plotted in Figure 4. For the case of an exponentially modulated light, ideally we would expect equally spaced events all occurring approximately simultaneously for all 9 neighboring pixels. However, we can see there is clearly some variation in the times at which events are generated in the pixels. We hypothesize this phenomena is explained by variations in the pixel response as is mentioned in [5]. However, answering this question is beyond the scope of this work. Here we simply introduce the reader to the nature of the response of the pixels of an event-based imager to exponentially increasing light.

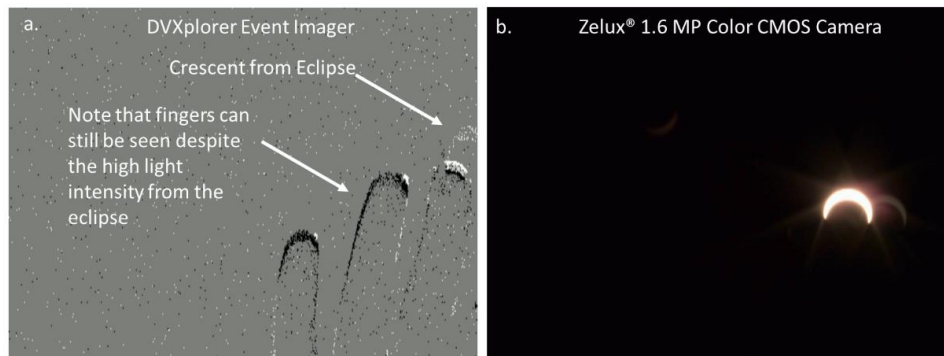


Figure 3 a.) Demonstration of the high dynamic range of event imagers (DVXplorer, 50 mm lens, 1.0 neutral density filter; b.) Demonstration of an 8 bit zelux 1.6 MP Color CMOS camera (0.6 and 3.0 neutral density filter used in series); in the context of imaging the 10/14/2023 eclipse as observed from Los Alamos, NM.

Exponentially Increasing Illumination on the Pixels of the DVXplorer

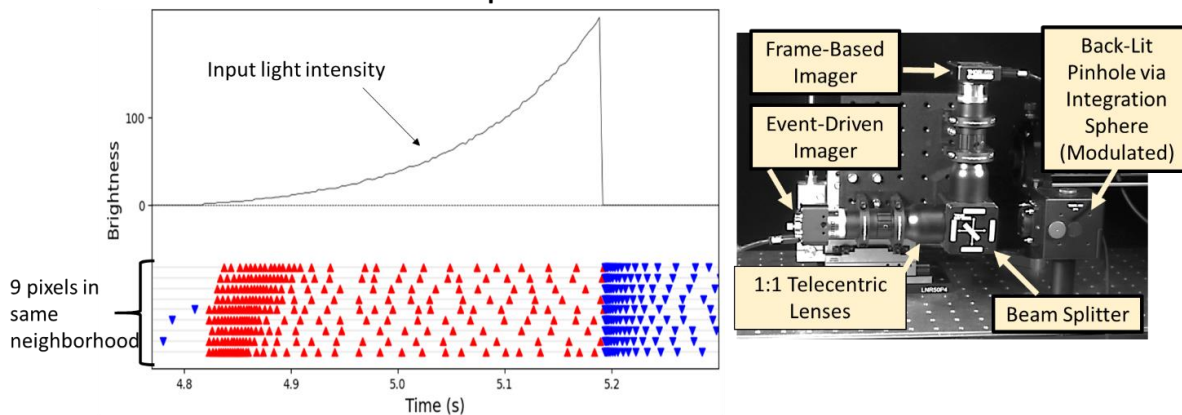


Figure 4 Example of the response of a DVXplorer event imager to a logarithmically increasing change in light intensity. Red, upward pointing triangle markers indicate positive event polarity and blue, downward pointing triangle markers indicate a negative event polarity. Right image shows associated experimental setup.

It is also noteworthy that neuromorphic sensors do not experience aliasing. This is because the event detection circuit inherently acts as a low-pass filter. If the physical phenomena being observed is changing faster than the event detection circuit can keep up with, the scene will appear to not change from the perspective of the circuit, and no events will be reported. This property is very attractive for fast dynamic processes such as those associated with additive manufacturing because it prevents dynamics faster than the frame-per-second capabilities of the imager, to corrupt the measurement.

In recent years there is increasing reason to consider event-based imagers for in-process monitoring of welding and additive manufacturing processes. Hayes et al demonstrated the potential [10] to use neuromorphic event-based imagers to characterize the dynamics of melt pools. To the best knowledge of the authors, the first reported use of a neuromorphic event imager to observe arc welding processes was provided by Gothard et al in [11]. This work provided evidence that neuromorphic event imagers possessed the dynamic range to observe the melt pool geometry and tungsten torch tip associated with a gas tungsten arc weld (GTAW). Furthermore, this work demonstrated a quantitative approach to converting event data to frame data that could potentially be fed to conventional image processing and computer vision pipelines. The high dynamic range properties of neuromorphic event-based imagers was further demonstrated by Mascareñas ([12]) in the context of both GTAW as well as laser welding. Analysis done in the course of this work further suggests that neuromorphic event imagers collect welding data in a far more efficient manner than conventional imagers and could potentially be compressed even further using techniques such as principle component analysis. Zheng et al demonstrated that event-based imagers could be used in an array processing mode for observing waves traveling along the top surfaces of liquids [13].

This work aims to further explore the potential for the use of event imagers for in-process monitoring of welding and additive manufacturing. This work focuses on the case of a laser welder being observed using an event-based imager.

Experimental Setup

This work focuses on the observation and analysis of a melt pool associated with laser welding using an event based imager. The laser welding setup is shown in Figure 5. In this case a weld is executed on a pipe sample of stainless steel material. A Davis 346 monochromatic neuromorphic event-driven imager ([8]) was used to observe the laser welding melt pool. The event imager used a microscope camera objective (UPC 709619589462 [14]). This microscope camera objective has a magnification of .7 to 4.5X and a working distance of 100mm to 115mm.

An example of an image of the laser melt pool captured using this setup is shown in Figure 5. An example of a melt pool observed using the event based imager is shown in Figure 6.

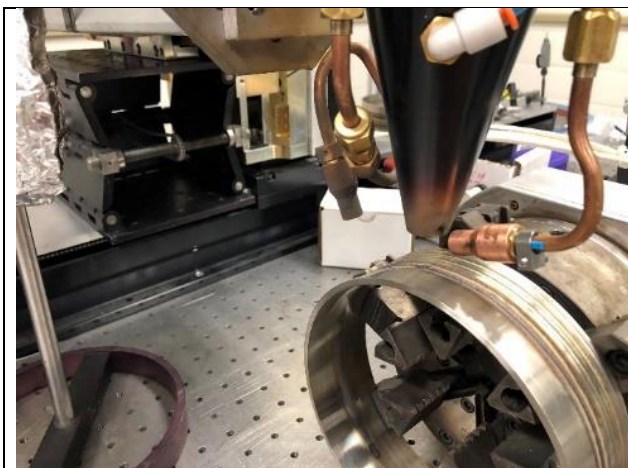


Figure 5 Laser welder which was under observation by an event imager.

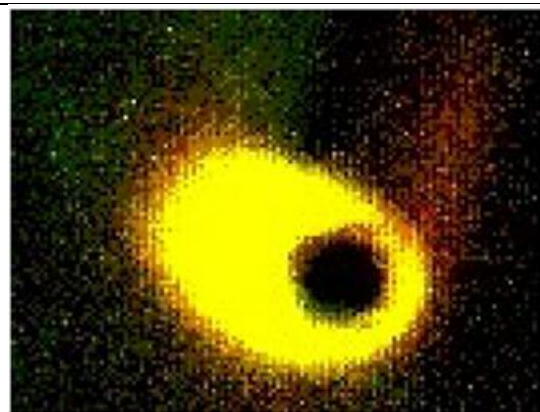


Figure 6 Event data naively summed into an image with an equivalent frame rate of 100 frames per second at 100% exposure time. Green pixels indicate positive polarity events, red pixels indicate negative polarity events, and yellow pixels indicate pixels where both positive and negative polarity events were detected.

Principle Components Analysis For Modeling and Tracking Melt Pool Shape

Figure 6 shows that the melt pool associated with laser welding has an elliptical nature to it. There is evidence to suggest that the shape of a melt pool can have an impact on the quality of the weld and the inclusion of porosity in the final weld [15]. Therefore we investigate the ability to model this elliptical shape using event-based imagery. Specifically, we focus on the use of the principle component analysis (PCA) algorithm ([16], [17]), to estimate the center and major/minor axes of a 2D ellipse that closely encloses the events associated with the melt pool within its boundary. The PCA-based workflow we have developed for analyzing and tracking the shape of the laser welding melt pool is shown in Figure 7. In this work we consider the case of performing 2D PCA over events bounded by windows in time. However, it should be noted that because 2D PCA has an analytical solution, it is possible to compute PCA in a streaming manner where the PCA solution can be updated for each new event that enters/leaves a fixed-length data buffer. In this way PCA can be implemented in a fast, streaming manner.

Event Processing Pipeline Description

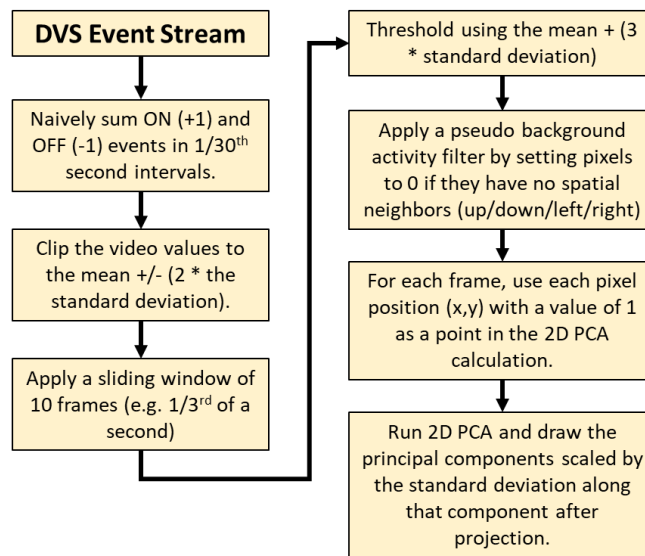


Figure 7 Signal processing workflow associated with using the principle component analysis algorithm on events generated from a melt pool.

Principle Components Analysis For Modeling and Tracking Melt Pool Shape - Results

We now consider the events measured using an event imager observing a laser welder melt pool. First, the 2D view of the spatio-temporal point cloud (2 spatial pixel dimensions, 1 temporal dimension) associated with the events generated by the laser-welder melt pool can be found in Figure 8 through Figure 9. Figure 10 shows a 3D view of the spatio-temporal point cloud of the events. These figures provide context for what event-based imagery of a melt pool looks like. Please note, event imagers can be very sensitive to change and can generate many events. Therefore, to facilitate viewing the events, only 1 in 500 of the events are displayed for a period of 10 seconds of laser welding. In these plots it is possible to observe the shape of the melt pool.

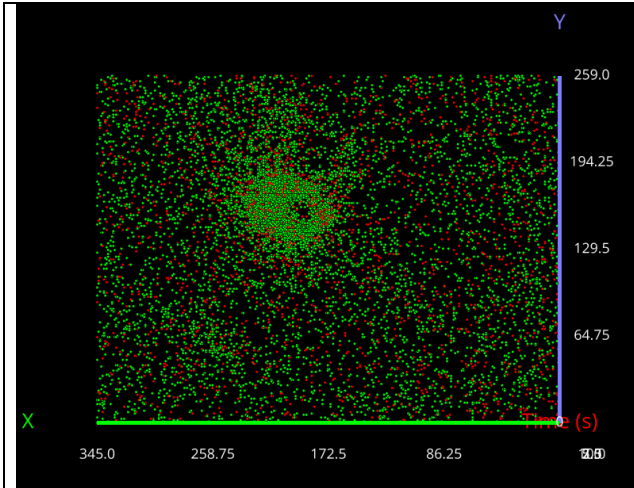


Figure 8 Spatio-temporal event point cloud for laser welding viewed along temporal axis.

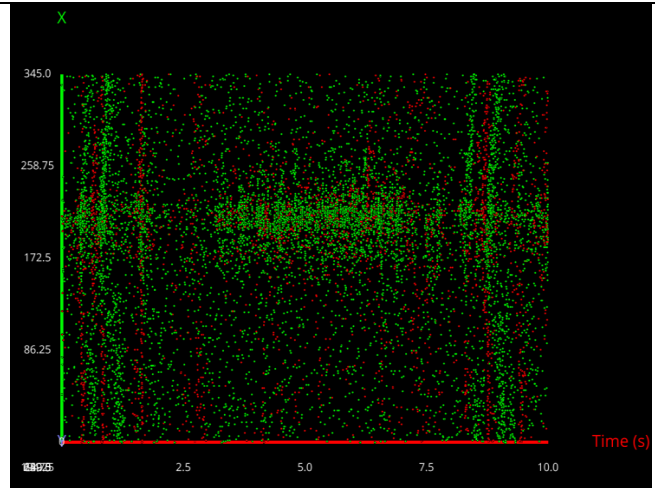


Figure 9 Spatio-temporal event point cloud for laser welding viewed along y pixel axis.

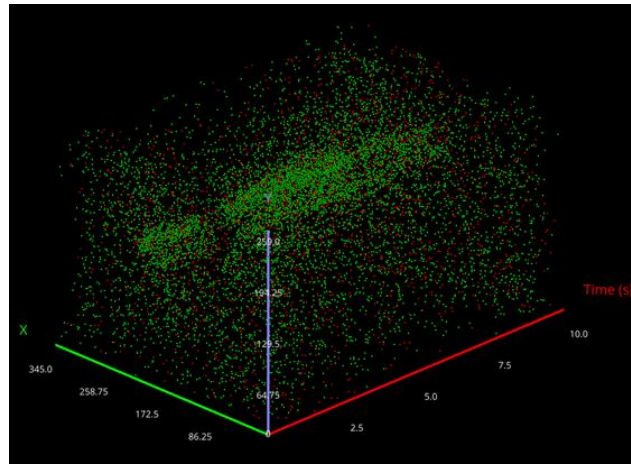


Figure 10 Spatio-temporal event point cloud for laser welding, isometric view.

Next, we apply the PCA tracking algorithm to the event data for a variety of different framerates in order to demonstrate the ability to estimate 2D elliptical models at different timescales. Snapshots associated with instants in time of the measurements, along with plots of the measured eigenvalues for each case are shown in Figure 12 - Figure 13 (STDV indicates the standard deviation). Please note that because the timescales of these plots vary, the time range over which events are considered decreases as well in order to display similar amounts of analysis results for each case. From these plots we can see that the PCA tracking algorithm shows promise for fitting relevant elliptical models to spatio-temporal event point clouds across a range of timescales relevant to laser welding and additive manufacturing, particularly at the slower timescales from 30 FPS to 300 FPS. Faster time scales appear to often local exhibit features that are smaller than the entire melt pool and are often not as well captured by an elliptical model and are not shown. Additional work should be done to learn appropriate models for the phenomena occurring at the faster timescales.

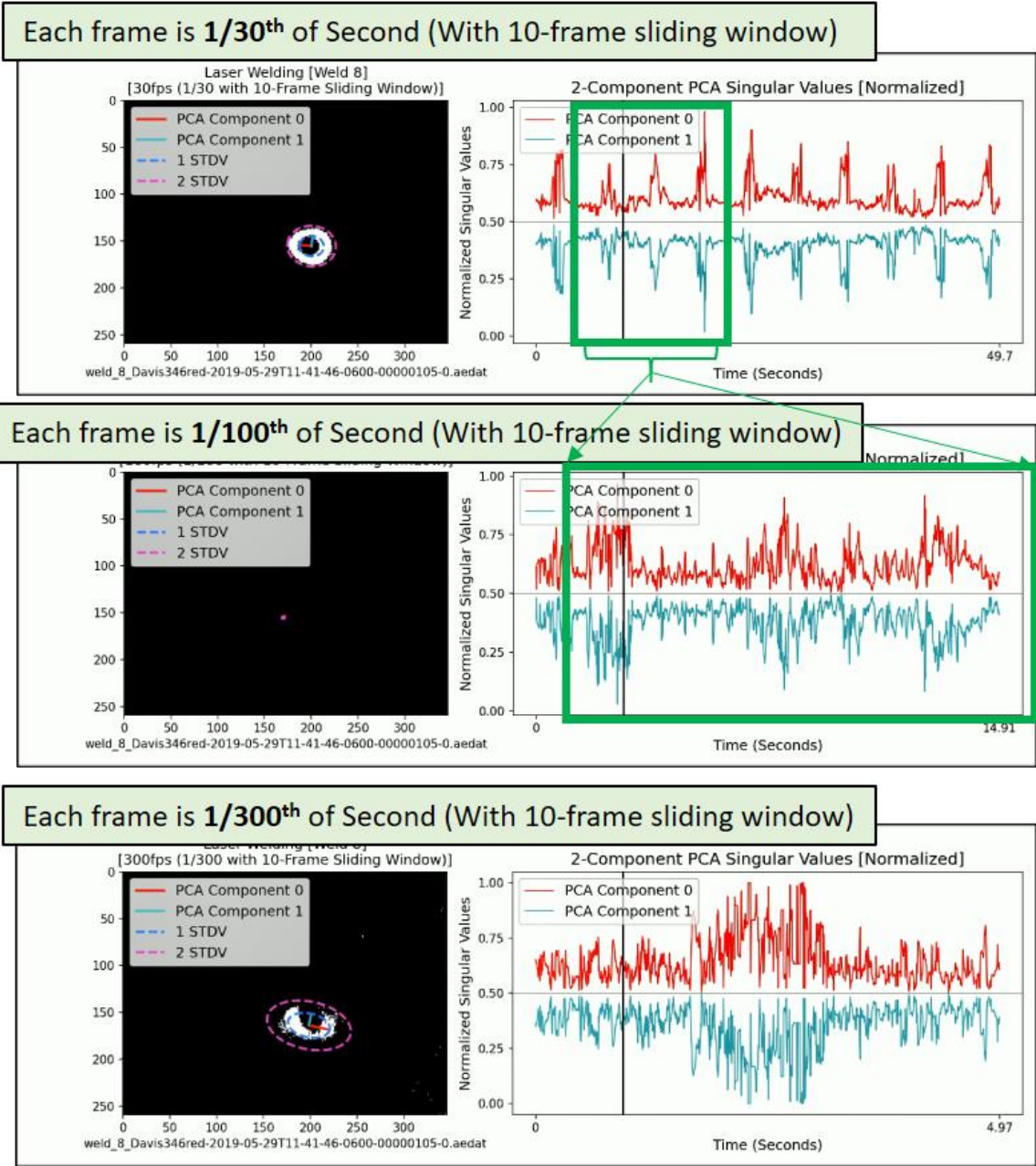
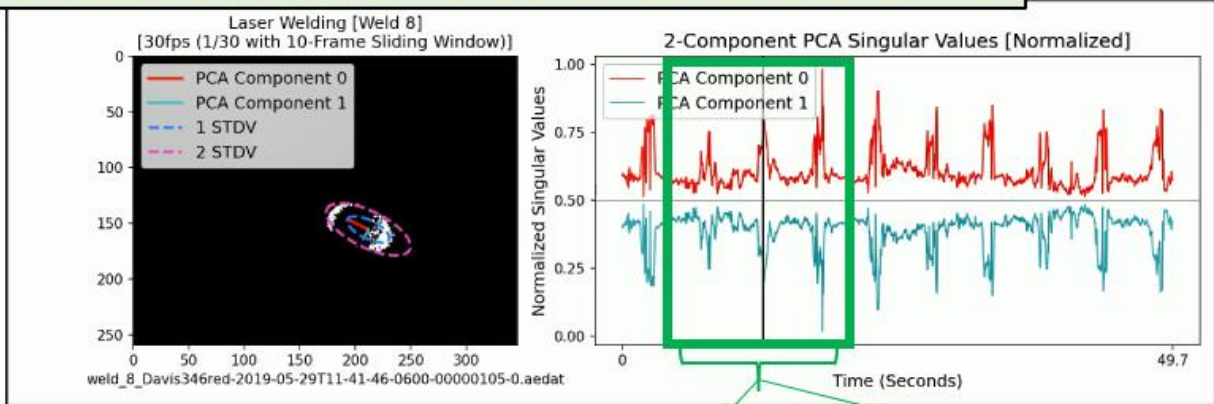
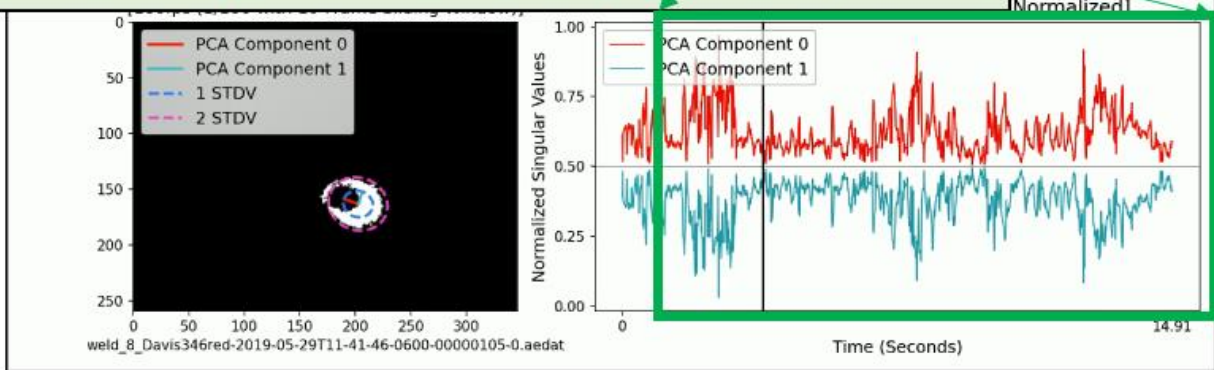


Figure 11 First example of PCA tracking approach and resulting eigenvalues for modeling the melt pool for specified framerate of 30, 100 and 300 frames per second.

Each frame is $1/30^{\text{th}}$ of Second (With 10-frame sliding window)



Each frame is $1/100^{\text{th}}$ of Second (With 10-frame sliding window)



Each frame is $1/300^{\text{th}}$ of Second (With 10-frame sliding window)

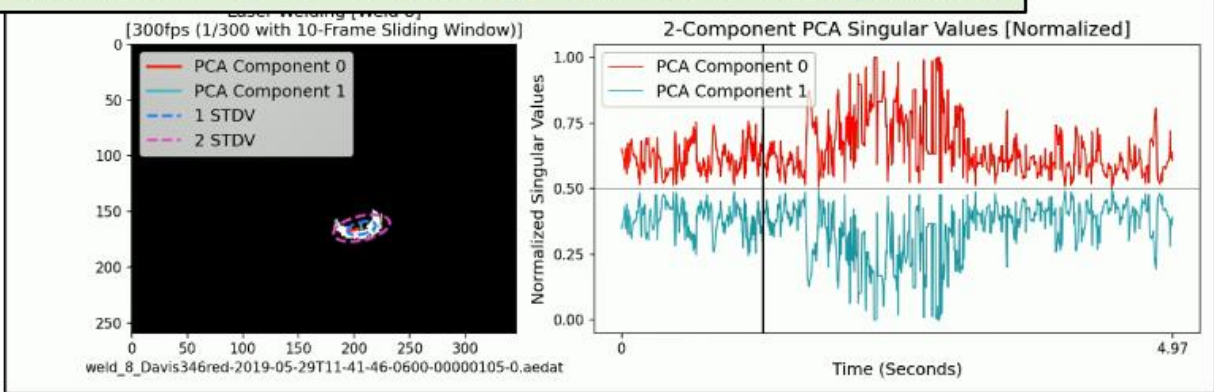


Figure 12 Second example of PCA tracking approach and resulting eigenvalues for modeling the melt pool for specified framerate of 30, 100 and 300 frames per second.

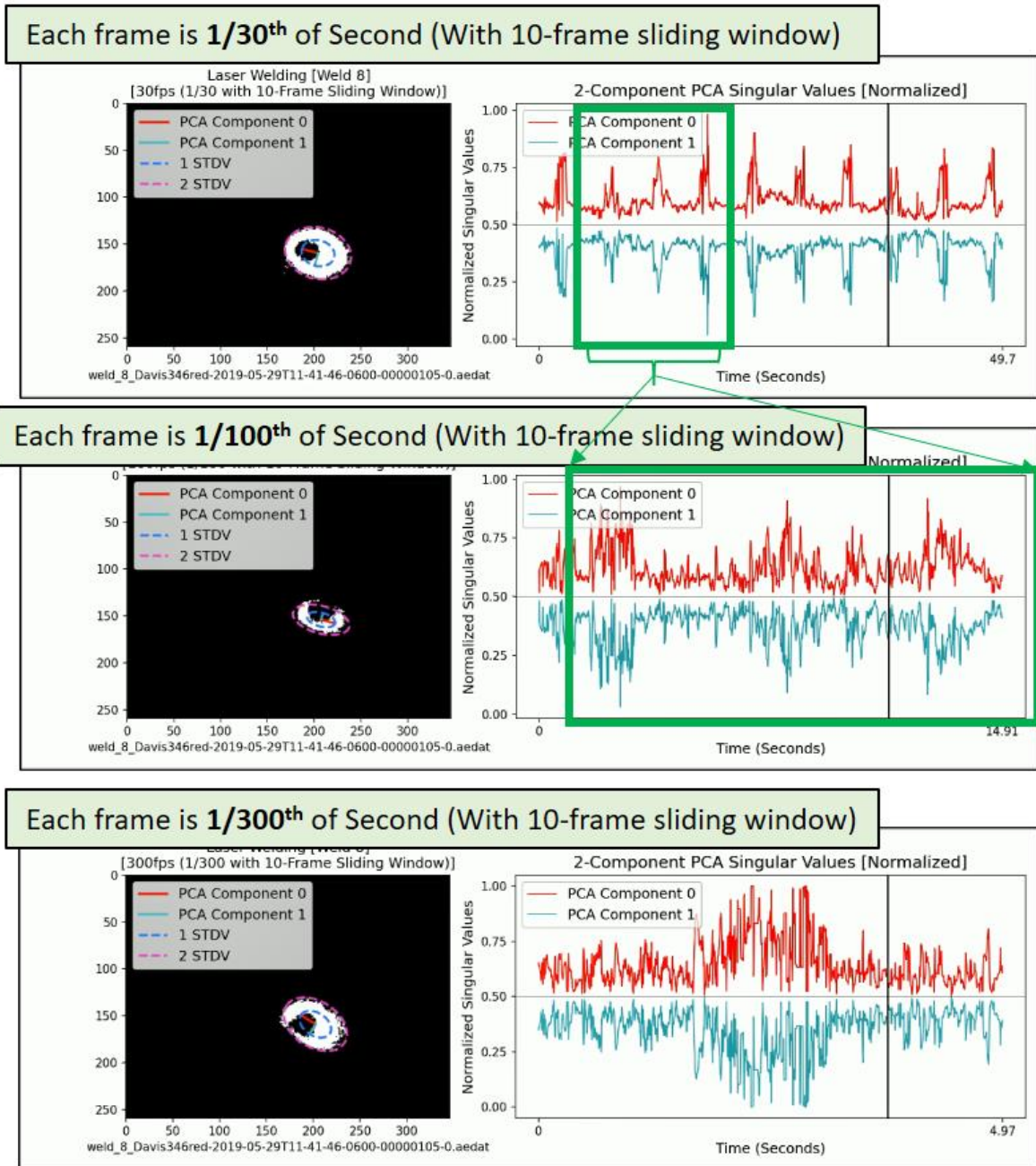


Figure 13 Third example of PCA tracking approach and resulting eigenvalues for modeling the melt pool for specified framerate of 30, 100 and 300 frames per second.

Conclusions

This work explores the possibility of using neuromorphic event-based imaging in the context of observing the geometry of melt pools and estimating an elliptical model for the shape of a melt pool. The initial results presented in this work suggest that high-speed, streaming elliptical model parameter estimation for melt pool shape from event imagers can be executed successfully over timescales relevant to laser welding. Neuromorphic event-based imagers have potential for monitoring melt pools for welding and additive manufacturing for 3 reasons. First, they have a high dynamic range. Second, they can detect phenomena on the millisecond to sub-millisecond timescale. Third, event-based imagers tend to generate less data than a conventional frame-based imager capturing data at a comparable framerate. The results presented in this work suggest that event-based

imagery has high potential to be used for in-process monitoring of welding and additive manufacturing and additional study into this area is warranted.

Acknowledgements

This paper was supported by the Laboratory Directed Research and Development program of Los Alamos National Laboratory under project number 20220494MFR, 20220426ER, 20190547MFR as well as other funding sources internal to Los Alamos National Laboratory. Los Alamos National Laboratory is operated by Triad National Security, LLC, for the National Nuclear Security Administration of US Department of Energy (Contract No. 89233218CNA000001). The DVS/DAVIS technology was developed by the Sensors group of the Institute of Neuroinformatics (University of Zurich and ETH Zurich), which was funded by the EU FP7 SeeBetter project (grant 270324). We would like to acknowledge the help of Amber Black and Michael Torrez with the data collection for this project.

References

- [1] Ashlee Vance, "A New Age of US Manufacturing Has Begun in California | Hello World with Ashlee Vance," Bloomberg Originals, 28 September 2023. [Online]. Available: <https://www.youtube.com/watch?v=IvDj-15ilRw>.
- [2] C. Mead and M. Ismail, Analog VLSI and Neural Systems, New York, NY: The Springer International Series in Engineering and Computer Science, 1989.
- [3] C. Mead, "Neuromorphic Electronic Systems," *Proceedings of the IEEE*, vol. 78, no. 10, pp. 1629-1636, 1990.
- [4] M. Mahowald and T. Delbruck, "Cooperative Stereo Matching Using Static and Dynamic Image Features," in *The Kluwer International Series in Engineering and Computer Science*, Springer, Boston, MA, 1989, pp. 213-238.
- [5] P. Lichtsteiner, P. C. and D. T., "A 128 x 128 120 dB 15 μ s Latency Asynchronous Temporal Contrast Vision Sensor," *IEEE J. Solid-State Circuits*, vol. 43, no. doi: 10.1109/JSSC.2007.914337, pp. 566-576, 2008.
- [6] G. Gallego, T. Delbruck, G. Orchard, C. Bartolozzi, B. Taba, A. Censi, S. Leutenegger, A. J. Davison, J. Conradt, K. Daniilidis and D. Scaramuzza, "Event-based Vision: A Survey," *IEEE Transactions on Pattern Analysis and Machine Intelligence*, vol. 40, no. 1, 2020.
- [7] Inivation, "Specifications - Current Models," 2022. [Online]. Available: <https://inivation.com/wp-content/uploads/2023/02/2022-09-iniVation-devices-Specifications.pdf>. [Accessed 12 May 2023].
- [8] Inivation, "DAVIS 346," 15 August 2019. [Online]. Available: <https://inivation.com/wp-content/uploads/2019/08/DAVIS346.pdf>. [Accessed 18 June 2024].
- [9] "Prophesee, Metavision for Machines," [Online]. Available: <https://www.prophesee.ai/>. [Accessed 3 January 2024].
- [10] C. Hayes, C. Schelle, G. Taylor, B. Martinez, G. Kenyon, T. Lienert, Y. Yang and D. Mascareñas, "Imager-Based Techniques for Analyzing Metallic Melt Pools for Additive Manufacturing," in *Conference Proceedings for the Society for Experimental Mechanics- International Modal Analysis Conference*, Orlando, FL, 2020.
- [11] A. Gothard, D. Jones, A. Green, M. Torrez, A. Cattaneo and D. Mascareñas, "Digital coded exposure formation of frames from event-based imagery," *Digital coded exposure formation of frames from event-based imagery*, vol. 2, no. 014005, 2022.

- [12] A. G. David Mascarenas, "Demonstration of Neuromorphic Event-Based Imagers for Optical Measurement of Melt Pools for Additive Manufacturing and Welding Diagnostics," in *International Modal Analysis Conference*, Orlando, FL, 2024.
- [13] K. Zheng, J. Sorenson, C. DeVilliers, A. Cattaneo, F. Moreu, G. Taylor and David Mascareñas, "Neuromorphic Data Processing for Event-Driven Imagery for Acoustic Measurements," in *International Modal Analysis Conference*, Orlando, FL, 2022.
- [14] HAYEAR, "Monocular Max 300x Zoom C-Mount Glass Lens Adapter F/Industry Digital Microscope Camera Objective," Amazon, [Online]. Available: https://www.amazon.com/Monocular-C-mount-Industry-Microscope-Objective/dp/B01CBCZPP4/ref=pd_sbs_421_5?_encoding=UTF8&pd_rd_i=B01CBCZPP4&pd_rd_r=8bd20f4e-f32c-11e8-ac33-170c9d662742&pd_rd_w=Ngg35&pd_rd_wg=PRI3T&pf_rd_i=desktop-dp. [Accessed 18 June 2024].
- [15] Q. Hayat, P. Franciosa, G. Chianese, A. Mohan, D. Ceglarek, A. Griffiths and C. Harris, "Elucidating the effect of circular and tailing laser beam shapes on keyhole necking and porosity formation during laser beam welding of aluminum 1060 using a multiphysics computational fluid dynamics approach," in *Proceedings of the International Congress of Applications of Lasers & Electro-Optics (ICALEO 2023)*, 2023.
- [16] K. Pearson, "On lines and planes of closest fit to systems of points in space," *Lond. Edinb. Dubl. Phil. Mag. J. Sci.*, vol. 2, no. 11, p. 559–572, 1901.
- [17] M. Greenacre, P. J. F. Groenen, T. Hastie, A. I. D’Enza, A. Markos and E. Tuzhilina, "Principal component analysis," *Nature Reviews Methods Primers*, vol. 2, no. 100, 2022.